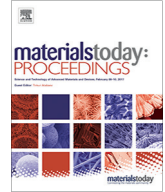




Contents lists available at ScienceDirect

Materials Today: Proceedings

journal homepage: www.elsevier.com/locate/matpr

Investigating impacts of FDM printing parameters and geometrical features on void formation in 3D printed automotive components

Yasaman Mohseni^{a,c}, Mina Mohseni^{a,d}, Sinduja Suresh^{a,b,c}, Marcello Riotto^e, Alka Jaggessar^{a,b}, J. Paige Little^{a,f}, Marie-Luise Wille^{a,b,c}, Prasad KDV Yarlagadda^{g,*}

^a School of Mechanical, Medical and Process Engineering, Queensland university of technology, 2 George Street, Brisbane 4000, Australia

^b Centre for Biomedical Technologies, Queensland University of Technologies, 2 George Street, Brisbane 4000, Australia

^c The Australian Research Council Industrial Transformation Training Centres (ARC ITTC) for M3D Innovation, Australia

^d The Australian Research Council (ARC) Training Centre for Cell and Tissue Engineering Technologies, Australia

^e Deputy GM Motor Trade Association of Queensland (MTAQ) and the Automotive Industry Skills Adviser at MTAQ, Logan road, Brisbane, Australia

^f Biomechanics and Spine Research Group, Centre for Children's Health Research, Queensland University of Technology, 62 Graham, South Brisbane, Australia

^g Dean (Engineering), University of Southern Queensland, Springfield Central Q, Brisbane 4300, Australia

ARTICLE INFO

Article history:

Available online xxxx

Keywords:

Additive manufacturing

Automotive industry

Manufacturing effects

Voids

Geometry of 3D printed component

ABSTRACT

Additive manufacturing (AM) has opened a world of new possibilities in the automotive industry by offering high flexibility in design, shortening production time, and producing lightweight and customizable parts. Despite these advantages, the high risk of defect formation associated with AM processes and the difficulty of defect detection in quality control stages have hindered the rapid adoption of AM in the automotive industry. Mechanical tests are destructive tests which are usually used for quality control of conventionally fabricated components. However, they are not practical for quality control of AM parts since, due to the higher risk of defects, a higher number of AM parts should be mechanically tested which is time-consuming and expensive. Hence, rather than destructive mechanical tests, automakers require non-destructive imaging techniques for AM parts to characterize defects for a high number of samples at the quality control stage. This study aims to examine the impact of printing parameters and geometrical features on the void formation of an automotive component (car window holder). These outcomes will be helpful in the establishment of non-invasive quality control for the window car holder which is based on imaging techniques. For this purpose, a window car holder was printed with varying printing parameters using the FDM technique. Based on the geometry of the component, two regions with distinct geometrical features were specified and analyzed using Micro-CT. Results indicate that by increasing printing speed (30 to 60 mm/min) and temperature (230 °C to 250 °C), voids fraction decreased. Conversely, when increasing the printing layer thickness (0.1 to 0.3 mm), the void fraction increased. It was also concluded that void formation in regions with curved surfaces and overhang structures is significantly higher compared to edges with an angle of 90 ° to 60 °. These results offer a platform to reduce the risk of defect formation in 3D-printed automotive parts, improving quality control.

Copyright © 2023 Elsevier Ltd. All rights reserved.

Selection and peer-review under responsibility of the scientific committee of the 16th Global Congress on Manufacturing and Management 2022. This is an open access article under the CC BY-NC-ND license (<http://creativecommons.org/licenses/by-nc-nd/4.0/>).

1. Introduction

Manufacturing industries are enthusiastic to utilize advanced techniques which facilitate producing complex parts with high quality while reducing material waste, cost, and time [1]. One of the popular production methods which have attracted attention

in different industries is an additive manufacturing (AM), known as 3D printing [2]. AM, which implements a transformative approach to industrial production, started in the 1960 s and has shown rapid and continual growth in different applications [2,3]. AM is a process for the fabrication of real 3D objects that creates parts by adding materials layer by layer based on a digital model [4,5]. The additive manufacturing technology was initially focused on the fabrication of small products or prototyping [6]. Since the last decade, AM has shown a growing trend for various purposes

* Corresponding author.

E-mail address: y.prasad@usq.edu.au (P.KDV Yarlagadda).

<https://doi.org/10.1016/j.matpr.2023.06.078>

2214-7853/Copyright © 2023 Elsevier Ltd. All rights reserved.

Selection and peer-review under responsibility of the scientific committee of the 16th Global Congress on Manufacturing and Management 2022.

This is an open access article under the CC BY-NC-ND license (<http://creativecommons.org/licenses/by-nc-nd/4.0/>).

as it offers several advantages compared to conventional fabrication methods [5].

In AM workflow, a 3D model is initially designed by Computer-Aided Design (CAD) software in STL (stereolithography) format and then sliced into layers with different thicknesses. The resulted G-code file is sent to the printer to control the printing toolpath, nozzle movement, and other printing parameters [7]. The G-code file is a text code which guides the printer and the nozzle movement for material deposition. This geometry-dependent fabrication workflow reduces the design limitations and gives the opportunity to go beyond simple models and create parts with more complex features.

AM process is very wide and includes very different techniques. Based on standards of the International Standardization for Organization (ISO) and the American Society for Testing and Materials (ASTM), all AM processes are divided into 7 general categories [8], namely: Vat photo polymerization [9], Material Jetting [10], Material extrusion [11,12], Binder Jetting [13,14], Powder Bed Fusion [15,16], Direct Energy Deposition [17], Sheet lamination [15]. Most of these AM techniques are according to layer upon layer [18]. The major differences between these techniques are how successive layers are made and what materials are used [19].

1.1. Additive manufacturing in the automotive industry

Automotive companies are continuously seeking technological revolutions which increase their production speed as well as improve the quality of finished parts to create more opportunities in this highly competitive market [20]. In the last decade, AM technology has recently attracted automakers' attention and is pushing the boundaries of the automotive industry by offering so many new possibilities, not achievable by conventional fabrication methods [21]. Additive manufacturing in the automotive industry facilitates prototyping and speeds up the design validation process, where components with new designs can be directly manufactured by AM with minimized tooling requirements. AM also allows precise design components and control of their macro and micro-structures. Automotive parts, especially internal components, often include internal channels, hidden features, thin walls, fine meshes, and complex curved surfaces [22]. These components, which work in extreme conditions and experience heat, moisture, and vibration, require accurate geometrical features for efficient functionality. Design flexibility as well as the accuracy of fabrication offered by AM make it possible to tailor these geometrical features and improve their long-term performance. AM is also a cost-effective way of prototyping, where new design ideas can be evaluated. One of the most critical advantages of AM in the automotive industry is reducing components' weight and therefore reducing fuel consumption. Using thermoplastic polymers rather than metals as well as optimizing the topology of components for less usage of material can significantly reduce the overall weight of components while improving their performance [23]. The materials which have been used in 3D printed automotive components are divided into four main groups including polymers, metals, ceramics, and composites. However, the current trend is towards polymer materials or reinforced polymer-based matrix as they reduce the overall weight of the component and have more flexibility to be shaped. In the last decade, the most common automotive components fabricated by AM technologies include interior parts, seats, tires, wheels, suspension, electronic items (such as sensors, and single-part control panels), exterior items (such as windbreakers and bumpers), framework, door, and some of the engine components [20]. Moreover, AM facilitates the manufacturing of large components and reduces assembly items by redesigning them as a single complicated component. This change significantly decreases the need for assembly tooling and therefore materials

usage and maintenance costs. It also reduces human involvement and associated errors which substantially increases the quality of final products. Additionally, additive manufacturing has created new horizons for manufacturers to communicate directly with customers and create customized components that have never existed before. It has enhanced automakers' abilities to design quickly and to save production time and cost when making personalized components for customers [24]. In traditional manufacturing methods, such as injection molding, each customized product required new molds and subsequent changes in the production line which made product customization highly time and cost-consuming.

1.2. FDM technique in the automotive industry

The fused Deposition Modelling (FDM) method is the most common AM technique for polymer-based products. It is a material extrusion technique where a polymer-based filament is pushed through a hot nozzle and deposited on a bed along a pre-designed pathway and eventually solidified [25]. This technique offers a simple and cost-effective fabrication method by heating and extruding thermoplastic polymers in a layer-by-layer fashion [26]. FDM technique has extensively attracted attention in automotive applications, where heavy metal parts can be replaced by 3D printed polymeric components. Currently, there is a high demand to reduce the weight of automotive components, and it seems that additively manufactured polymeric components, feasible by FDM, are a great substitute for metals. The most common materials for FDM parts in the automotive industry are Acrylonitrile butadiene styrene (ABS), Polylactic acid or Polylactide (PLA), Polycarbonate (PC), and Polyurethane (PU) which are ideal candidates for lightweight automotive components which require complex structures and high mechanical strength [27].

1.3. Manufacturing defects associated with FDM

Despite the huge benefits of FDM and the growing interest of automakers in using FDM, the difficulty of defect detection which put the functionality and quality of products at the risk has hindered the rapid adoption of this technique in the automotive industry. Layer delamination and voids are major manufacturing defects which have attracted attention due to their high effect on the mechanical properties of the final part [28]. Air traps in 3D printed parts are a common manufacturing defect that affects the technical functionality of products [29,30]. This defect may be relevant to pre-existing air bubbles in the raw materials or may be associated with the manufacturing process and parameters [31,32]. In the first case, the quality of the chosen material is the first source of defect formation during printing. Hence, passing the required quality control window of materials play an integral role in decreasing of deformation of defects. In the FDM technique, the presence of voids in filaments is an example of defects associated with raw material which causes unavoidable defects in the final product [33]. In the second case, in the FDM technique, the printing strategy should be optimized to minimize the risk of air trap [33,34]. Take an example, the shape of the nozzle in the FDM technique results in creating manufacturing defects [35]. With a circular nozzle, the extrusion of a rectangular line of molten material is almost impossible. Hence, the cross-sections do not form sharp corners, and placing many filaments alongside each other creates an almost uniform pattern of voids.

Lack of efficient bonding between layers is another common manufacturing defect in AM techniques that reduces the quality of fabricated parts and further increase the risk of the presence of inevitable voids [34]. These defects impact the mechanical performance of components significantly. Even small defects can hugely diminish the mechanical performance of 3D-printed com-

ponents in the long term and negatively affect the whole system. Previous studies showed that layer bonding can decrease mechanical properties by 50% of FDM parts [36]. The other disadvantage of these defects is losing isotropic properties which are highly critical for rotational components, especially at high speed.

Mechanical tests are the major quality tests for the evaluation of conventionally fabricated components. A higher chance of defect formation makes the quality control of 3D printed parts more difficult as a higher number of samples should be mechanically tested. On the other hand, mechanical tests are destructive methods, where the component are failed under different loading conditions. Because of the higher chance of defect formation and the need for more 3D printed samples which should be mechanically tested, these destructive tests are impractical for the evaluation of 3D printed parts. Therefore, automakers require non-destructive imaging techniques to examine defects for quality control in 3D-printed parts. In this regard, a good understanding of how geometrical features impact defect formation in vulnerable regions is essential. This research attempts to investigate the deep knowledge of effect of printing parameters including layer height, speed nozzle, printing temperature and geometrical features on the voids formation of 3D printed parts in the automotive industry.

2. Method and materials

2.1. Measure and prepare CAD model

A car window holder as an automotive component has been used in this study (Fig. 1). All the dimensions of the conventionally fabricated component were measured by a calliper. The CAD model was designed by Solidwork and imported as the STL file format into the slicing software, Cura (Ultimaker). 100% infill density with a Line pattern was chosen to slice the model (Fig. 2).

Different printing parameters such as speed nozzle (S), printing temperature (T), and layer thickness (L) were set according to Table 1 based on the literature review [37,38 39,40]. The G-Code files were sent one at a time to the LulzBot Mini 2 Desktop (MINI2) to fabricate the specimens with 3 repeats. Acrylonitrile Butadiene Styrene (ABS) was used.

2.2. Micro-CT

3D printed samples were inspected by an X-ray microcomputed tomography (Micro-CT) tool to detect manufacturing defects. Each sample was scanned 2 times using Micro-CT (SCANCO Medical AG, Brütisellen, Switzerland). Micro-CT as a non-invasive method allows the investigation of the whole structure of 3D printed products according to the emission of X radiations. Initially, printed samples are put on the appropriate tube which is compatible with the samples' size as holder type (48 mm). The X-ray scan is carried out with the best resolution of 14 μm (voxel size), where is achieved the

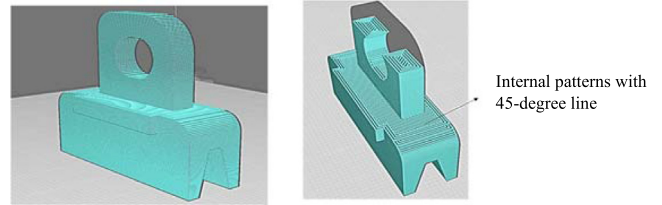


Fig. 2. The solid model was sliced in Cura using the linear pattern with 45°.

Table 1

The printing parameters which have been considered so far.

Parameters	Minimum	Maximum
Speed Nozzle (mm/min)	S = 30	S = 60
Printing Temperature °C	T = 230	T = 250
Layer Thickness (mm)	L = 0.1	L = 0.3

best quality. The setting of 45 KV for voltage, 0.1 mm AL (PMMA) for calibration and filter AL 0.1 mm is used during scanning. The Micro-CT scans these two different critical regions for all 3D printed components. At the end of the scan, the 3D data from the set of X-ray images which are obtained by the CT- scan is fulfilled by means of reconstruction software. The volume of interest for evaluation, by drawing contour lines to choose the threshold and the regions which are interested in the scan are identified. Therefore, a 3D reconstruction by applying a threshold for imaging analysis of CT scan results is needed to use a threshold for analyzing defects. All images were first exported as DICOM files for 3D visualization. The images were then analysed using the Scanco evaluation program.

To save the inspection time and scan data size for automotive components which are usually large, only the critical areas including overhang structures and curve surfaces which are critical in load bearing and are more vulnerable to manufacturing defects can be inspected and scanned. For the car window holder component, there are three different critical regions which are included bottom, middle and top. In this study, two critical regions which are (343 slices) are specified by reference lines in the Micro-CT and analysed (Fig. 3). To create boundaries and define the first and second critical regions respectively, reference lines from the end of the component upwards to 5 mm high and from the middle of the circle upwards to 5 mm be specified and scanned in the Micro-CT.

2.3. Defect analysis in FDM printing

Before analysing manufacturing defects such as voids, data segmentation is needed. Segmentation specifies the interface between solid materials and surrounding air. Each segmentation allocates a

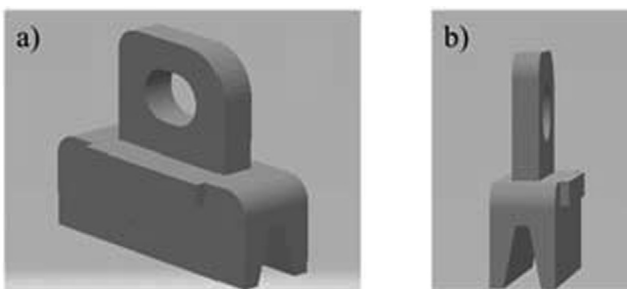


Fig. 1. The car window holder CAD model prepared in Solidwork. a) Perspective view, b) Side view.

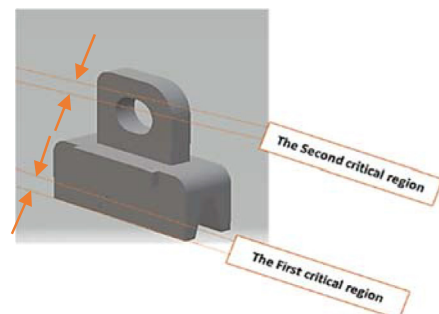


Fig. 3. The critical regions.

label to each pixel of the image, which determines the area or material of the pixel. The software used to detect manufacturing defects is commonly known as image segmentation software. In this study, the Avizo software version 9.5.0 is used to visualize, analyse and inspect 3D printed components which are scanned by Micro-CT. Different steps have been described to detect the voids and analyse the 3D printed samples in a productive way (Fig. 4).

Specifying Threshold: Initially, when the data is set in Avizo analysis, there is not a clear phase between the pixels associated with the material and the background. Hence, the appropriate threshold should be chosen to separate the regions that need to be analysed (Fig. 5(a)). Thresholding is a process of dividing a colored or grey image into different sections, where the scanned image is segmented based on whether the pixel values are greater or lower than the threshold. Therefore, an appropriate threshold should be chosen to distinguish the background and material from each other.

Filtering Process: Filtering is used to remove the noise from the selected material or structure. In this process, the selection starts from a seed point and continues to all connected pixels with similar color intensity. Therefore, the noises which do not connect to the materials are not selected and therefore disappear from our selection (Fig. 5(b)).

Voids Detection: In the next step, the selected material is filled in a new label and subtracted from the previously selected material in the old label to specifically distinguish voids. This step shows a clear process of the subtraction and the voids which were detected (Fig. 6).

Voids analysis: For calculating voids fraction at each region, the volume of voids is divided by the volume of the selected material.

$$\text{VoidsFraction} = \frac{\text{Voids volume}}{\text{Material volume}}$$

3. Results and discussion

To have a better understanding of how voids fraction is changing between samples with different printing parameters, the samples were divided into three groups, where each group has two constant parameters and one variable parameter as indicated in Table 2 and Fig. 7. The variable parameters in groups 1, 2, and 3 are respectively Nozzle Speed (S), Printing Temperature (T), and Layer Thickness (L).

Critical Regions: For every three groups, the voids was detected, and voids fraction was calculated by Avizo software. Table 3 shows voids fraction values in all samples at regions 1 and 2 respectively.

In order to have a simple comparison between voids fraction between three groups of two regions, the graphs shown in Fig. 8 was also prepared for region 1 and 2 respectively. Also, the standard error has been calculated which can be seen in these graphs.

Critical region 1: In the first critical region, the voids fraction is reduced by increasing the temperature as well as speed, while it is reduced by the detected reduction of the layer thickness. In group 1, as the speed is increased from 30mm/min to 60mm/min, the voids fraction is decreased with a nearly constant rate between

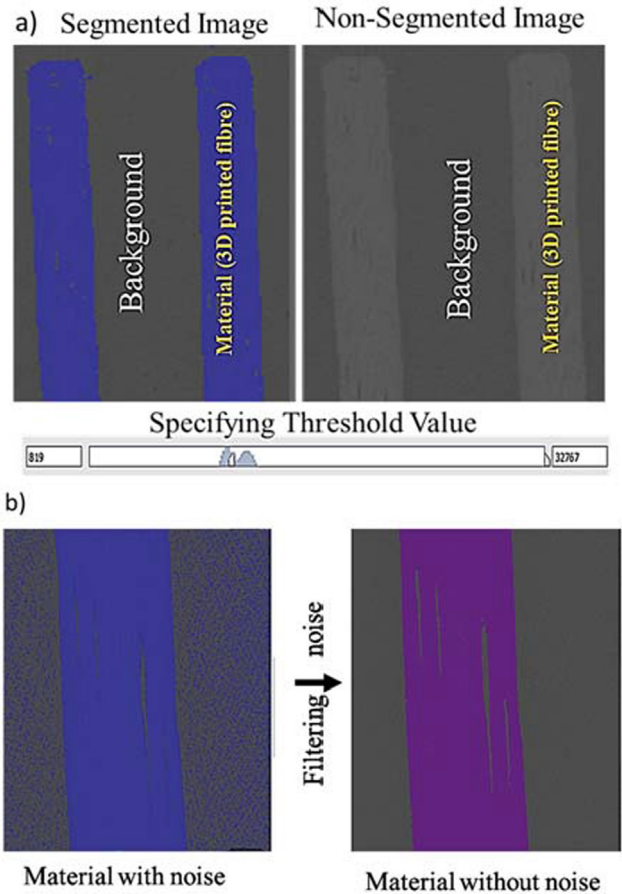


Fig. 5. a) the image was segmented by choosing a proper threshold range, where the material is distinguished from the background. b) filtering process is used to remove the noise.

all samples. In group 2, where the temperature is increased from 230 °C to 250 °C, the voids fraction of samples generally decreased. However, the samples with a smaller layer thickness ($L = 0.1 \text{ mm}$) show a more significant reduction. In group 3, the volume fractions of samples are considerably impacted by the layer thickness as the changes are more significant than in the other two groups. By increase of layer thickness from 0.1 mm to 0.3 mm, the volume fractions have been increased.

Critical Region 2: The same trend which exists in region 1 is also observed in the second region. Totally, by boosting the speed nozzle and temperature the range of voids fraction is decreased, whereas this range is increased by enhancing the layer thickness. In group 1 as the speed is increased from 30 mm/min to 60 mm/min, the voids fraction is decreased. In group 2, as the temperature is increased from 230 °C to 250 °C, the voids volume of the samples is decreased. In group 3, all the samples show an increase as the layer thickness is increased from 0.1 mm to 0.3 mm. Likewise, in region 1, the highest speed, temperature, and the lowest layer thickness cause the minimum voids fraction in region 2.



Fig. 4. Different processes which should be followed to analyze voids.

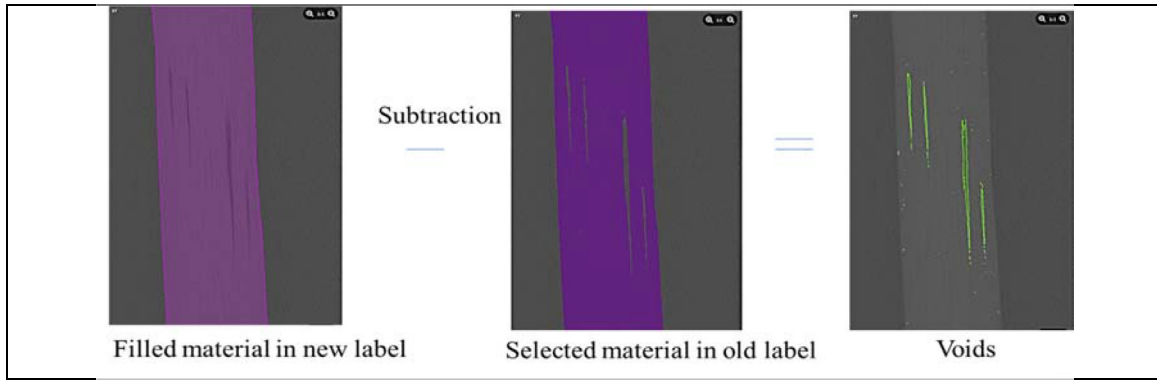


Fig. 6. Filled material is subtracted from the initially selected material to distinguish the voids.

Table 2

Samples have been analysed and divided into three groups for comparison.

	Constant parameters	Variable parameters
Group 1	Printing Temperature / Layer thickness	Nozzle Speed
Group 2	Nozzle Speed / Layer Thickness	Printing Temperature
Group 3	Nozzle Speed / Printing Temperature	Layer Thickness

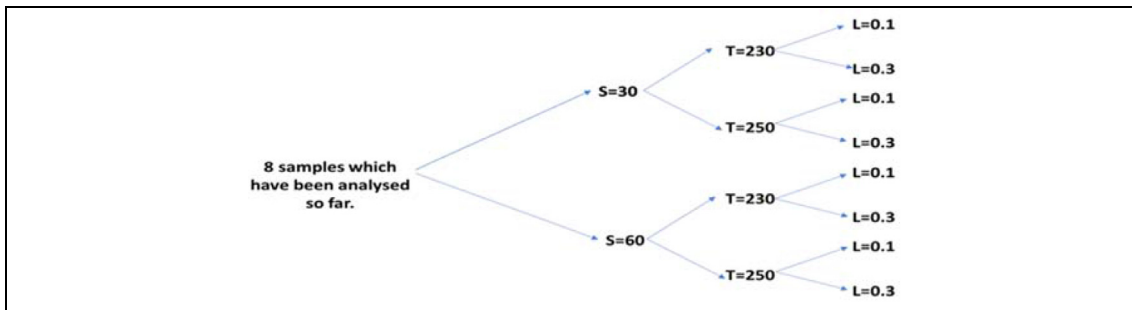


Fig. 7. 8 samples have been analysed at each group. Speed (S), Temperature (T), Layer Thickness (L).

Table 3

Voids fraction which is calculated for the samples using Avizo software. A) Region 1, B) Region 2.

		T=250	T=250	T=230	T=230
		L=0.3	L=0.1	L=0.3	L=0.1
Group 1	S=30	0.0141	0.00455	0.0149	0.0082
	S=60	0.0122	0.00295	0.0130	0.00615
		S=60	S=60	S=30	S=30
Group 2		L=0.3	L=0.1	L=0.3	L=0.1
	T=230	0.0130	0.00615	0.0149	0.0082
	T=250	0.0122	0.00295	0.0141	0.00455
		S=60	S=60	S=30	S=30
		T=250	T=230	T=250	T=230
Group 3	L=0.1	0.00295	0.00615	0.00455	0.0082
	L=0.3	0.0122	0.0130	0.0141	0.0149
		S=60	S=60	S=30	S=30
	T=250	T=230	T=250	T=230	
	L=0.1	0.0044	0.00585	0.00565	0.0066
	L=0.3	0.01165	0.0144	0.01295	0.015

A)

B)

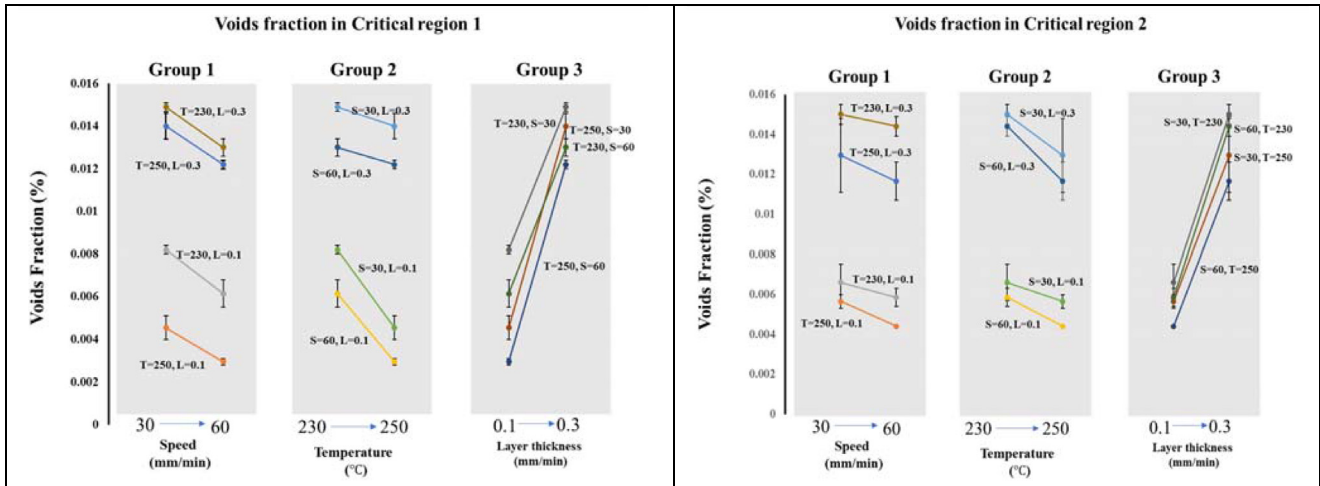


Fig. 8. Voids fraction in region 1 and 2 for group 1, 2, and 3.

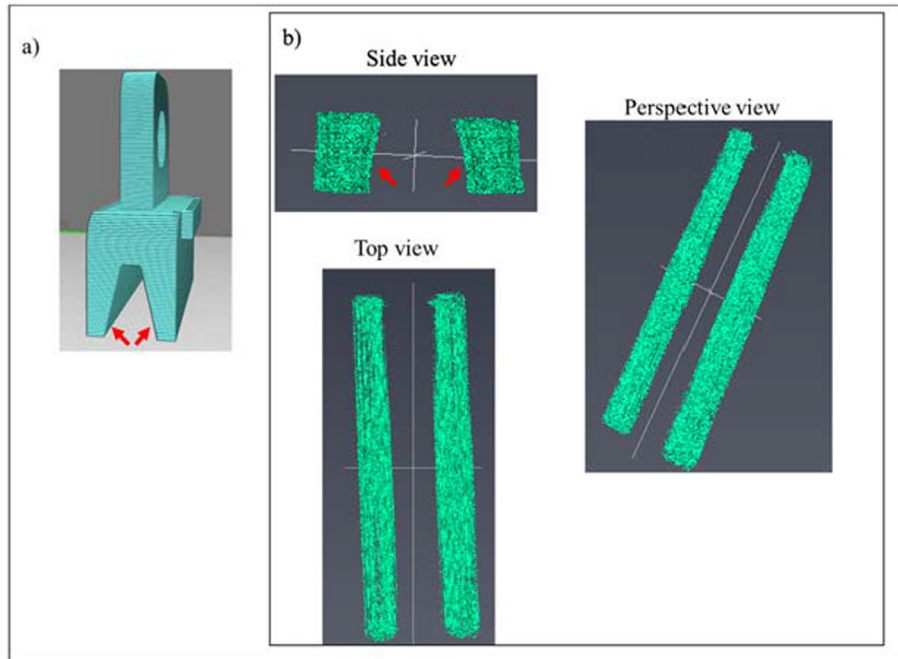


Fig. 9. a) the sliced model of the component with red arrow showing the edge with an angle of 60°. b) The Micro-CT images of region 1 at different views with the same density of voids. (For interpretation of the references to color in this figure legend, the reader is referred to the web version of this article.)

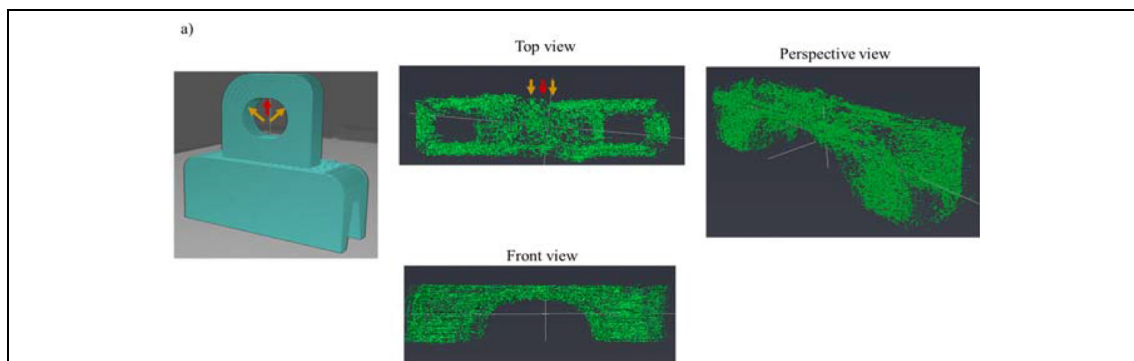


Fig. 10. a) the sliced model of the component with red arrow showing the overhanging spot and a yellow arrow showing the curvy surfaces. b) the micro-ct images of region 2 at different views. (For interpretation of the references to color in this figure legend, the reader is referred to the web version of this article.)

The relation between voids formation and geometrical features: As indicated in Fig. 9, region 1 is mainly a non-overhanging structure. The only difficult spot from a printing perspective is the edges which have been shown with red arrow and have an angle of 60° (Fig. 9 (a)). As observed from Micro-CT images, these edges are not showing a difference in voids density when are visually compared with other spots (Fig. 9 (b)). Voids density which can be seen with green spots are completely same at region 1. Therefore, it can be concluded this region has a roughly a uniform void distribution.

In contrast to region 1, region 2 has overhanging structures and curvy surfaces which result in a higher number of pores. Fig. 10 indicates overhanging structure, red arrow, and curve surface, yellow arrows, of region 2. As observed from Micro-CT results, these surfaces have a higher density of pores while the middle regions are almost free of voids.

4. Conclusion and future work

In this study, we have designed and manufactured the car window holder as an automotive component with FDM technique. Three different printing parameters are taken into consideration. This study summarises the impact of printing parameters such as layer height, speed nozzle and printing temperature of FDM printed polymeric material and the geometrical feature of the component on voids as a manufacturing defect. By using Micro-CT and Avizo software, it is found that with increasing speed and temperature, voids fraction decreases, while increasing layer thickness leads to increased voids fraction in regions 1 and 2. Moreover, the minimum range of volume fraction for the 3D printed sample belongs to the highest speed nozzle ($S = 60 \text{ mm/min}$), highest printing temperature ($T = 250 \text{ }^\circ\text{C}$), and the minimum layer thickness ($L = 0.1 \text{ mm}$). Micro-CT provides the precise characterization of the voids fraction. Two critical regions were analysed with more details to find out the relation between geometrical features and manufacturing defects. According to Micro-CT images, void formation regions with curved surfaces is significantly higher compared to edges with an angle of 90 to 60. In the future, the sensitivity of different regions to printing parameters and Comparison of the average of voids fraction of all samples in region 1, and 2 will be analyzed. Additionally, the other critical region of the car window holders with curves and overhangs will be taken into consideration for a complete comparison.

CRedit authorship contribution statement

Yasaman Mohseni: Writing – original draft, Conceptualization, Data curation, Formal analysis, Software. **Mina Mohseni:** Writing – review & editing, Methodology, Software. **Sinduja Suresh:** Writing – review & editing, Methodology, Software. **Marcello Riotto:** Writing – review & editing, Supervision. **Alka Jaggesar:** Supervision. **J. Paige Little:** Writing – review & editing. **Marie-Luise Wille:** Supervision. **Prasad KDV Yarlagadda:** Supervision.

Data availability

Data will be made available on request.

Declaration of Competing Interest

The authors declare that they have no known competing financial interests or personal relationships that could have appeared to influence the work reported in this paper.

Acknowledgment

This work has been supported by the Australian Research Council Industrial Transformation Training Centres (ARC ITTC) for M3D.

All 3D printed samples have been printed in the Queensland University of Technology lab. The authors would also like to thank Melissa Johnston for helping to print samples.

References

- [1] F. Calignano, D. Manfredi, E.P. Ambrosio, S. Biamino, M. Lombardi, E. Atzeni, et al., Overview on additive manufacturing technologies, *Proc. IEEE* 105 (2017) 593–612.
- [2] J.K. Min, B. Mosadegh, S. Dunham, S.J. Al'Aref, *3D Printing applications in cardiovascular medicine*, Academic Press, 2018.
- [3] T. Caffrey, T. Wohlers, and I. Campbell, "Executive summary of the Wohlers Report 2016," ed: Loughborough University, 2016.
- [4] M. Savastano, C. Amendola, and E. Massaroni, "3-D printing in the spare parts supply chain: an explorative study in the automotive industry," in *Digitally supported innovation*, ed: Springer, 2016, pp. 153-170.
- [5] C.K. Chua, C.H. Wong, W.Y. Yeong, Standards, quality control, and measurement sciences in 3D printing and additive manufacturing, Academic Press, 2017.
- [6] S. Saleh Alghamdi, S. John, N. Roy Choudhury, N.K. Dutta, Additive manufacturing of polymer materials: Progress, promise and challenges, *Polymers* 13 (2021) 753.
- [7] F. Alkadi, K.-C. Lee, A.H. Bashiri, J.-W. Choi, Conformal additive manufacturing using a direct-print process, *Addit. Manuf.* 32 (2020).
- [8] A. Nazir, K.M. Abate, A. Kumar, J.-Y. Jeng, A state-of-the-art review on types, design, optimization, and additive manufacturing of cellular structures, *Int. J. Adv. Manuf. Technol.* 104 (2019) 3489–3510.
- [9] X. Chen, G. Zhao, Y. Wu, Y. Huang, Y. Liu, J. He, et al., Cellular carbon microstructures developed by using stereolithography, *Carbon* 123 (2017) 34–44.
- [10] L. Cheng, P. Zhang, E. Biyikli, J. Bai, J. Robbins, A. To, Efficient design optimization of variable-density cellular structures for additive manufacturing: theory and experimental validation, *Rapid Prototyp. J.* (2017).
- [11] R.C. Rumpf, J. Pazos, C.R. Garcia, L. Ochoa, R. Wicker, 3D printed lattices with spatially variant self-collimation, *Prog. Electromagn. Res.* 139 (2013) 1–14.
- [12] M.K. Ravari, M. Kakhodaei, M. Badrossamay, R. Rezaei, Numerical investigation on mechanical properties of cellular lattice structures fabricated by fused deposition modeling, *Int. J. Mech. Sci.* 88 (2014) 154–161.
- [13] D. Snelling, Q. Li, N. Meisel, C.B. Williams, R.C. Batra, A.P. Druschitz, Lightweight metal cellular structures fabricated via 3D printing of sand cast molds, *Adv. Eng. Mater.* 17 (2015) 923–932.
- [14] A. Druschitz, C. Williams, D. Snelling, M. Seals, Additive manufacturing supports the production of complex castings, in: *In Shape Casting: 5th International Symposium 2014*, 2014, pp. 51–57.
- [15] I. Gibson, D. W. Rosen, B. Stucker, M. Khorasani, D. Rosen, B. Stucker, et al., *Additive manufacturing technologies* vol. 17: Springer, 2021.
- [16] M. Leary, M. Mazur, J. Elambasseril, M. McMillan, T. Chirent, Y. Sun, et al., Selective laser melting (SLM) of AlSi12Mg lattice structures, *Mater. Des.* 98 (2016) 344–357.
- [17] A. Plotkowski, O. Rios, N. Sridharan, Z. Sims, K. Unocic, R. Ott, et al., Evaluation of an Al-Ce alloy for laser additive manufacturing, *Acta Mater.* 126 (2017) 507–519.
- [18] M.R. Khosravani, T. Reinicke, On the environmental impacts of 3D printing technology, *Appl. Mater. Today* 20 (2020).
- [19] R. Ranjan, D. Kumar, M. Kundu, and S. C. Moi, "A critical review on Classification of materials used in 3D printing process," *Materials Today: Proceedings*, 2022.
- [20] R. Leal, F. Barreiros, L. Alves, F. Romeiro, J. Vasco, M. Santos, et al., Additive manufacturing tooling for the automotive industry, *Int. J. Adv. Manuf. Technol.* 92 (2017) 1671–1676.
- [21] G. Dwivedi, S.K. Srivastava, R.K. Srivastava, Analysis of barriers to implement additive manufacturing technology in the Indian automotive sector, *Int. J. Phys. Distrib. Logist. Manag.* (2017).
- [22] S.G. Sarvankar, S.N. Yewale, Additive manufacturing in automobile industry, *Int. J. Res. Aeronaut. Mech. Eng.* 7 (2019) 1–10.
- [23] A. García-Domínguez, J. Claver, and M. A. Sebastián, "Integration of Additive Manufacturing, Parametric Design, and Optimization of Parts Obtained by Fused Deposition Modeling (FDM). A Methodological Approach," *Polymers*, vol. 12, p. 1993, 2020.
- [24] D. Jankovics, A. Barari, Customization of automotive structural components using additive manufacturing and topology optimization, *IFAC-PapersOnLine* 52 (2019) 212–217.
- [25] Y. Chen, X. Peng, L. Kong, G. Dong, A. Remani, R. Leach, Defect inspection technologies for additive manufacturing, *Int. J. Extreme Manuf.* 3 (2021).
- [26] M. Heidari-Rarani, N. Ezati, P. Sadeghi, and M. Badrossamay, "Optimization of FDM process parameters for tensile properties of polylactic acid specimens using Taguchi design of experiment method," *Journal of Thermoplastic Composite Materials*, p. 0892705720964560, 2020.

- [27] A. Bouzouita, "Elaboration of polylactide-based materials for automotive application: study of structure-process-properties interactions," Université de Valenciennes et du Hainaut-Cambresis; Université de Mons, 2016.
- [28] C. Bellehumeur, L. Li, Q. Sun, P. Gu, Modeling of bond formation between polymer filaments in the fused deposition modeling process, *J. Manuf. Process.* 6 (2004) 170–178.
- [29] M. Seidl, J. Habr, J. Bobek, J. Šafka, and L. Běhálek, "Mechanical properties of products made of abs with respect to individuality of fdm production processes," 2017.
- [30] D. Croccolo, M. De Agostinis, G. Olmi, Experimental characterization and analytical modelling of the mechanical behaviour of fused deposition processed parts made of ABS-M30, *Comput. Mater. Sci.* 79 (2013) 506–518.
- [31] K. Günaydın and H. S. Türkmen, "Common FDM 3D printing defects," in *International Congress on 3D Printing (Additive Manufacturing) Technologies and Digital Industry*, 2018.
- [32] A. Yadav, P. Rohru, A. Babbar, R. Kumar, N. Ranjan, J.S. Chohan, et al., Fused filament fabrication: a state-of-the-art review of the technology, materials, properties and defects, *Int. J. Interact. Des. Manuf. (IJIDeM)* (2022) 1–23.
- [33] S. Wickramasinghe, T. Do, P. Tran, FDM-based 3D printing of polymer and associated composite: A review on mechanical properties, defects and treatments, *Polymers* 12 (2020) 1529.
- [34] M. Baechle-Clayton, E. Loos, M. Taheri, H. Taheri, Failures and flaws in fused deposition modeling (FDM) additively manufactured polymers and composites, *J. Compos. Sci.* 6 (2022) 202.
- [35] P. Ferretti, C. Leon-Cardenas, G.M. Santi, M. Sali, E. Ciotti, L. Frizziero, et al., Relationship between fdm 3d printing parameters study: Parameter optimization for lower defects, *Polymers* 13 (2021) 2190.
- [36] A.Y. Al-Maharma, S.P. Patil, B. Markert, Effects of porosity on the mechanical properties of additively manufactured components: A critical review, *Mater. Res. Express* 7 (2020).
- [37] B. Zharylkassyn, A. Perveen, D. Talamona, Effect of process parameters and materials on the dimensional accuracy of FDM parts, *Mater. Today: Proc.* 44 (2021) 1307–1311.
- [38] M. Chaudhari, B.F. Jogi, R. Pawade, Comparative study of part characteristics built using additive manufacturing (FDM), *Procedia Manuf.* 20 (2018) 73–78.
- [39] G. Ćwikła, C. Grabowik, K. Kalinowski, I. Paprocka, P. Ociepka, The influence of printing parameters on selected mechanical properties of FDM/FFF 3D-printed parts, in: in *IOP conference series: materials science and engineering*, 2017, p. 012033.
- [40] X. Li, R. Cui, L. Sun, K.E. Aifantis, Y. Fan, Q. Feng, et al., 3D-printed biopolymers for tissue engineering application, *Int. J. Polym. Sci.* 2014 (2014).